EUROPEAN FUSION DEVELOPMENT AGREEMENT

EFDA–JET–PR(03)24

R. Sartori, G. Saibene, L.D. Horton, M. Becoulet, R. Budny, D. Borba, A. Chankin
G.D. Conway, G. Cordey, D. McDonald, K. Guenter, M.G. von Hellermann,
Yu. Igithkanov, A. Loarte, P.J. Lomas, O. Pogutse, J. Rapp
and JET EFDA contributors

Study of Type III ELMs in JET

Study of Type III ELMs in JET

R. Sartori[1], G. Saibene[1], L.D. Horton[2], M. Becoulet[3], R. Budny[4], D. Borba[5], A. Chankin[6], G.D. Conway[2], G. Cordey[7], D. McDonald[7], K. Guenter[7], M.G. von Hellermann[8], Yu. Igithkanov[9], A. Loarte[1], P.J. Lomas[7], O. Pogutse[7], J. Rapp[10] and JET EFDA contributors*

[1]EFDA Close Support Unit, Garching, 2 Boltzmannstrasse, Garching,DE
[2]Association Euratom-IPP, MPI fur Plasmaphysik, 2 Boltzmannstrasse, Garching (DE)
[3]Association Euratom-CEA, CE Cadarache, F-13108 St.Paul-lez-Durance, CEDEX, F
[4]PPPL, PrincetonUniversity, PO.Box 451, Princeton, NJ 08543 (USA)
[5]Associacao EURATOM/IST, Centro de Fusao Nuclear, 1096 Lisbon, CODEX, Portugal
[6]Japan Atomic Energy Research Institute, Naka-machi, Naka-gun, Ibaraki-ken, Japan
[7]EURATOM-UKAEA Fusion Association, Culham Science Centre, Abingdon, OX14 3DB, UK
[8]FOM-Rijnhuizen,Ass.EURATOM-FOM,TEC,PO Box 1207,3430 BE Nieuwegein,NL
[9]Max-Planck-Institute for Plasma Physics, Teilinstitut Greifswald, EURATOM Ass., D17491, Greifswald, Germany
[10]EFDA Close Support Unit, Culham, Abingdon, Oxon, OX14 3DB, UK
** See annex of J. Pamela et al, "Overview of Recent JET Results and Future Perspectives", Fusion Energy 2000 (Proc. 18th Int. Conf. Sorrento, 2000), IAEA, Vienna (2001).*

Preprint of Paper to be submitted for publication in
Plasma Physics and Controlled Fusion

ABSTRACT.

This paper presents the results of JET experiments aimed at the study of the operational space of plasmas with a Type III ELMy edge, in terms of both local and global plasma parameters. In JET, the Type III ELMy regime has a wide operational space in the pedestal ne-Te diagram, and Type III ELMs are observed in standard ELMy H-modes as well as in plasmas with an Internal Transport Barrier (ITB). The transition from an H-mode with Type III ELMs to a steady state Type I ELMy H-modes requires a minimum loss power, $P_{TypeI} \bullet P_{TypeI}$ decreases with increasing plasma triangularity. In the pedestal n_e-T_e diagram, the critical pedestal temperature for the transition to Type I ELMs is found to be inversely proportional to the pedestal density ($T_{crit} \propto 1/n$) at low density. In contrast, at high density T_{crit} does not depend strongly on density. In the density range where $T_{crit} \propto 1/n$, the critical power required for the transition to Type I ELMs decreases with increasing density. Experimental results are presented suggesting a common mechanism for Type III ELMs at low and high collisionality. A single model for the critical temperature for the transition from Type III to Type I ELMs, based on the resistive interchange instability with magnetic flutter, fit well the density and toroidal field dependence of the JET experimental data. On the other hand, this model fails to describe the variation of the Type III n_e-T_e operational space with isotopic mass and q_{95}. Other results are instead suggestive of a different physic for Type III ELMs. At low collisionality, plasma current ramp experiments indicate a role of the edge current in determining the transition from Type III to Type I ELMs while at high collisionality, a model based on resistive ballooning instability well reproduces, in term of a critical density, the experimentally observed q_{95} dependence of the transition from Type I to Type III ELMs. Experimental evidence common to Type III ELMs in standard ELMy H-modes and in plasma with ITB indicates that they are driven by the same instability.

1. INTRODUCTION

Type III ELMy H-modes are commonly observed in all divertor Tokamaks. In comparison with the Type I ELMy regime, these ELMy H-modes are characterised by small high frequency ELMs and by reduced energy confinement (10-30%). The Type III ELMy regime represents a limit to the operational space of Type I ELMs. In fact, at high density, the transition from Type I to Type III ELMs limits the density achievable with good confinement. Moreover, the transition to Type III ELMs also defines the minimum power below which Type I ELMs are no more observed.

In plasmas with an internal transport barrier, the benefit (in term of the divertor transient power load) of a Type III ELMy edge is combined with the transport reduction in the core plasma. In JET, this regime is achieved at relatively low pedestal density compared to the Greenwald density and the pedestal collisionality of those plasmas is low ($\nu^* < 5\ 10^{-2}$). In those conditions, keeping the edge in the Type III ELMy regime and avoiding transition to Type I ELMs is an issue, since large Type I ELMs can interact with the internal transport barrier causing its "erosion'[1].

The reference scenario for Q=10 inductive operation in ITER is a standard ELMy H-mode with

Type I ELMs. This operating point will be relatively near to the Type III operational boundary [2]. Therefore, the study of the operational space of Type III ELMs and its scaling with machine and plasma parameter is important for the control and/or the avoidance of those ELMs. This paper reports the results of experiments carried out in JET to study the operational space of Type III ELMs. Those experiments were carried out in the standard ELMy H-modes regimes, but the results will be compared with the findings for plasmas with an internal transport barrier. The operational space of Type III ELMs is studied in terms of global plasma parameters, such as input power, plasma density, toroidal field, and plasma triangularity (these findings are reported in sections 2 an 3) as well as in terms of the pedestal parameters n_e and T_e (section 4). The dedicated experiments described in this paper were carried out with the JET Mark II Gas Box (GB) divertor. The results of previous JET experiments with the Mark IIA divertor [3] are consistent, both in terms of the behaviour of global and local parameters, with the results described here, but one significant difference is also observed. The comparison between the GB and Mark IIA results is shortly discussed in Section 5. In Section 6, the JET experimental data are compared with some theoretical models for Type III ELMs. The results of this comparison are discussed highlighting common features and differences between the Type III ELMs with and without an internal transport barrier, and between Type III ELMs at high and low pedestal collisionality. Finally, Section 7 is dedicated to the analysis of the energy confinement of the Type III ELMy H-modes and to briefly discuss the reasons and extent of the confinement degradation with respect to the Type I ELMy regime.

2. THE POWER THRESHOLD FOR TYPE I ELM

ELMy H-modes with Type III ELMs are observed at low power above the predicted L-H threshold power, $P_{L\text{-}H} = 0.45\, n_e^{0.75} B_t R^2$, [4]. According to the definition given in [5, 6], in H-modes with Type III ELMs the ELM frequency f_{ELM} decreases with increasing input power. Fig 1 and Fig.2 illustrate the typical features of a power scan in JET, for Neutral Beam heated ELMy H-modes without any external gas fuelling. In this example the plasma current, I_p, was 2.5MA, the toroidal field, B_t, was 2.4T ($q_{95} \cong 3$). The plasma average triangularity, δ, was $\cong 0.22$.

In the power scan of Fig.1 the input power P_{IN} is increased in steps, starting from P_{IN} just above $P_{L\text{-}H}$. At the lowest input powers ($P_{IN} \leq 7$MW in Fig.1) the plasma is in the Type III ELMy regime, which is characterised by high frequency ELMs with low D_α amplitude. At slightly higher input power (P_{IN}=8.8MW in Fig.1), the plasma might access the Type I ELM regime and sometimes maintain it for several energy confinement times, but permanent (relative to the heating pulse length) or cyclic transitions to the Type III ELM regime are observed. One of such “permanent” transitions to Type III ELMs is shown in Fig 1 (second box): the discharge with 8.8MW NBI has a period of Type I ELMs which is followed by a transition to the Type III ELMy regime. This transition is accompanied by a large decrease in density and stored energy. At higher P_{IN} (10MW, again in Fig.1) a steady state Type I ELMy H-mode is achieved. ”Steady state” means, in this context, that the ELM type, the average diamagnetic stored energy $\langle W_{DIA} \rangle$ (average over the ELM period), and

the average plasma density are constant for the entire duration of the additional heating period. In those conditions, the input power is equal to the average loss power, $<P_{loss}>=P_{IN}-<dW_{DIA}/dt>$.

In Fig 2, the ELM repetition frequency f_{ELM} is plotted as a function of input power for the discharges of Fig.1 and some additional discharges with the same plasma parameters. For P_{IN} less than ≅8MW, f_{ELM} decreases with increasing P_{IN} (Type III ELMs) while for P_{IN} greater than ≅10MW f_{ELM} increases with input power (Type I ELMs). The plasma discharge with a transition from Type I to Type III is characterised, in the plot of f_{ELM} versus power, by two values of f_{ELM} for a given input power. The Type I ELM frequency of this plasma corresponds to the minimum of the Type I ELM frequency versus power (Fig 2). In other words, Type I ELMy H-modes with minimum TypeI ELM frequency are difficult to achieve in steady state. According to the general behaviour of the ELM type and ELM frequency versus power illustrated in Fig. 1 and Fig. 2, one can define "power threshold for Type I ELMs", PTypeI, as the lowest input power PIN necessary to maintain in steady state (as defined above) an ELMy H-mode with Type I ELMs. (P_{TypeI}≅10MW in the example of Fig.1 and Fig. 2).

Fig.3 illustrates that long additional heating pulse duration (long compared to the energy confinement time) and small increments in P_{IN} (small compared to the threshold power) are important for the determination of P_{TypeI}. Fig.3 shows the D_α trace for two power scans in 2MA/2T plasma and with different plasma triangularities: δ≅0.25 and δ≅0.33. For those power scans, the steps in power were smaller than the ones in the example of Fig 1 and 2, and the heating pulse duration was longer (8s as opposed to 5s). As indicated by the vertical line in Fig.3, with 5s of additional heating, the estimated power required to maintain Type I ELMs for the entire duration of the heating pulse would have been =30% lower. Fig.3 also shows that, as P_{IN} is increased, the transitions from Type I to Type III become cyclic, i.e. Type I ELMs are recovered at constant P_{IN}, and the total period with Type III ELMs becomes shorter. In fact, for example, the discharge with 5.9MW (δ≅0.25), is in the Type I ELMy regime only for 8% of the pulse duration, as opposed to the discharge with 7.6MW NBI, which has Type I ELMs for 65% of the pulse duration. In summary, steady state Type III ELMs are observed at low power above the L-H threshold power and steady state Type I ELMy H-modes are only observed above a critical power, P_{TypeI}. There is an intermediate range of power where phases with Type I and Type III ELMs coexist. In this range of power, the duration of the phases with Type III ELMs decreases with increasing P_{IN}.

Results from previous experiment carried out with the Mark IIA divertor [3] already suggested that P_{TypeI} can be empirically expressed as a multiple of the predicted L-H threshold power P_{L-H}, or, in other words, that the parametric dependence of P_{TypeI} on n_e and B_t might be similar to the one of the L-H threshold power. A dedicated experiment to study the proportionality between P_{L-H} and P_{TypeI} was carried out with the JET Mark II Gas Box (GB) divertor [7]. The results of this experiment are summarised in Fig.4. In the experiment, power scans were carried out with Neutral Beam Injection (NBI) in plasmas with different I_p and B_t and at a fixed triangularity, δ≅0.25. In a Type I ELMy Hmode with NBI, there is a minimum density that can be achieved. This density, called

"natural" density, is the steady state density achieved without external gas fuelling, as in all the experiments described above. At low triangularity, ´"E0.2, the natural density is "E50% of the Greenwald density limit, nG. As a consequence of the proportionality between natural density and Ip, the predicted L-H threshold power increases with Ip. In the experiment summarised in Fig.4 Ip was varied from 2 to 3 MA (2, 2.5 and 3MA) at Bt of 2.4T, and a power scan was carried out for each value of Ip. Similarly, at Ip=2.5MA PIN was varied in plasmas with Bt increased to 3T. In Fig.4 the input power and predicted threshold power of steady state H-modes with Type I ELMs are compared with the same quantities in the initial Type I ELMy phase of plasmas where cyclic or permanent transitions to the Type III ELM regime are observed.. As shown in the figure, the results of this experiment confirms the previous findings that an H-mode with Type I ELMs at low triangularity can be maintained in steady state when the input power is about twice the predicted L-H threshold power: PTypeI"E 2PL-H.

In this experiment I_p and n_e are not independent variables. Therefore, the proportionality of P_{TypeI} with P_{L-H} could be due to either I_p or n_e dependence. Separate experiments [8] showed that the L-H threshold power does not depend on I_p. The observed proportionality between P_{TypeI} and P_{L-H} suggests that also P_{TypeI} depends on density rather than on I_p. The result of this experiment on the proportionality between P_{L-H} and P_{TypeI} is consistent with the inverse mass dependence of both the L-H threshold power [9] and the power required for the transition to the Type I ELMy regime [9,10]. The multiplication factor between P_{TypeI} and P_{L-H} exhibits some day-to-day variation ($\approx$ +/-20% in GB, for similar additional heating pulse duration), suggesting a yet not quantified dependence on additional variables, generally referred to as an "effect of vessel conditioning".

Although the proportionality between P_{TypeI} and P_{L-H} is a useful global empirical scaling, Fig.1 already shows that this scaling does not give a complete picture of the experimental results. In fact, the time evolution of the ratio P_{IN}/ P_{L-H} that follows the transition from Type I to Type III ELMs seems to be in contradiction with the picture of a simple proportionality between P_{TypeI} and P_{L-H} (Fig.1, plasma with P_{IN}=8.8MW: black traces). As shown in Fig.1, a large decrease in plasma density is observed at the transition from the Type I to the Type III ELMy regime. As the density decreases, so does the predicted P_{L-H} ($\propto n^{0.75}$), and the ratio P_{IN}/ P_{L-H} increases to values greater than 2. As a consequence, the H mode should in principle recover the Type I ELMy behaviour. Fig.1 shows that this is not the case. It will be shown in section 4 that this apparent contradiction might be explained in terms of local variables and could also be related to the deviation of the L-H threshold power, at low density, from the predicted density scaling.

3. THE EFFECT OF PLASMA TRIANGULARITY ON THE POWER THRESHOLD FOR TYPE I ELMS

ELMy H-modes with different triangularity have different steady state parameters. In particular, the natural density increases with δ, being 70 to 80% of n_G for $\delta\cong$0.3-0.4 [11], compared to 50% at $\delta\cong$0.2. Moreover, the ELM frequency decreases with increasing δ. The higher natural density at

high δ implies, at fixed input power, a lower margin above the L-H threshold power than at low δ. As a consequence, from the proportionality between P_{TypeI} and P_{L-H} one would expect that high triangularity plasmas should require higher power for steady state Type I ELMs. On the contrary, the results of experiments with the Mark IIA divertor already suggested that P_{TypeI} could be lower at high δ than at low δ. The variation of P_{TypeI} with δ was investigated in detail with the GB JET divertor [12]. The experiment was carried out at 2MA/2T, using NBI heating, with plasma triangularity of 0.25 and 0.33. The D_α traces for some of the discharges in this experiment are shown in Fig.3. In the power scan at δ =0.33 P_{TypeI} is 7.6MW, compared to the 9MW necessary to maintain Type I ELMs at δ=0.25. The experiment shows that the power threshold for Type I ELMs decreases with increasing δ: $P_{TypeI} \cong 2.2\ P_{L-H}$ at δ=0.25 and $P_{TypeI} \cong 1.8$ PL-H at δ=0.33. A similar result, but with a different I_p/B_t combination (2.5MA/2.4T) is shown in Fig 4. The lower values of the ratio P_{IN}/P_{L-H} for this earlier experiment could be due to the shorter pulse length (≅5s) that was used.

Although in those steady H-mode plasmas the average stored energy is constant, W is not constant on the time scale of the ELM period: on this timescale the loss power is reduced by the power required to re-heat the plasma in between ELMs ($P_{loss}=P_{IN}-dW_{DIA}/dt$). For similar plasma parameters, the ELM frequency decreases for increasing δ and dW_{DIA}/dt in between ELMs (approximated here as $\Delta W_{DIA}/\Delta t$), is also lower for the high δ plasmas. Therefore, the loss power required for steady state Type I ELMs could in principle be similar at high and low δ since both P_{IN} and dW_{DIA}/dt decrease with increasing δ. What is observed is instead that the minimum P_{loss} necessary for a steady state Type I ELMy H-mode is lower at high δ and the minimum power to the separatrix is also lower. These observations indicate that the lower P_{TypeI} at high δ is not related to the variation of the ELM frequency with δ.

Figure 5 shows the ELM frequency as a function of the NBI input power for the high and low triangularity power scans of Fig 3. The dotted lines indicate discharges that have periods both of Type I and of Type III ELMs, i.e. a double value of f_{ELM} for given P_{IN}. The interval of power where this mixed ELM behaviour is observed gives an indication of the extent of the input power range where steady state plasmas with Type I ELMs are not achievable and of the possible error in the determination of P_{TypeI}, due to short pulse length.

In JET high density ELMy H-modes, it has been shown [13] that the power required to access a regime of good confinement at high density (mixed Type I-II ELMs, [14]) decreases with higher plasma triangularity. Therefore, the reduction of the power threshold for Type I ELMs with triangularity is observed, in ELMy H-modes, over the entire density range.

4. LOCAL PARAMETERS - H-MODE OPERATIONAL SPACE

4.1 OBSERVATION OF TYPE III ELMS AT LOW AND HIGH PEDESTAL DENSITY

In this paper we refer to the Type III ELMs described in the previous sections as “low density Type III ELMs”. In fact, in those low power Type III ELMy H-modes with no external gas fuelling the normalised density is typically only 25-30% of n_G. At high density and higher input power, a

transition to Type III ELMy H-modes typically occurs when, at constant PIN, the density of an H mode with Type I ELMs is increased by gas fuelling [11,15]. Therefore, from an operational point of view, low density Type III ELMs are observed in plasmas with no external fuelling at low input power above the L-H threshold power. The transition to the Type I ELMy regime is obtained by increasing P_{IN} and thus the margin above P_{L-H}. At high density, the back transition from Type I ELMs to Type III ELMs occurs when the margin over P_{L-H} is decreased by increasing the density, at constant and relatively high input power. Similarly to low density Type III ELMs, the repetition frequency of high density Type III ELMs decreases with increasing P_{IN}-P_{rad} [11].

At low density, in H-mode plasmas where a transitions from the Type I to the Type III ELMy regime occurs (minimum of Type I ELM frequency), as well as in steady state Type I ELMy plasmas with input power just above P_{TypeI}, a "compound" structure is often observed in the D_α trace after the Type I ELM crash (see Fig.1). Type I ELMs with these characteristics are often called in JET "compound ELMs". In plasmas with compound ELMs, the large D_α spike of the Type I ELM is followed by a short period of more frequent ELMs with lower D_α amplitude. Those frequent ELMs have a D_α signature similar to Type III ELMs. Moreover, the density and stored energy behaviour that follows the Type I ELM crash is similar to the one at the transition from Type I to Type III ELMs. Therefore we assume here that compound ELMs are a very short periods of Type III ELMs that follow a Type I ELM, although the power dependence of f_{ELM} is difficult to verify, since compound ELMs occur in a narrow power range and non-stationary conditions.

High frequency, low amplitude ELMs with a D_α signature similar to Type III ELMs are also observed in discharges with simultaneous internal transport barrier, ITB [16] and H-mode edge transport barrier. The frequency and amplitude of these ELMs is often anti-correlated with the internal transport barrier strength, as shown in Fig.6. Those low amplitude ELMs are observed in plasmas with ITB with an input power much higher than P_{TypeI} for standard ELMy H-modes, but lower than the power required for Type I ELMs in the same regime [1,17]. As in standard Type I ELMy H-modes, in ITB plasmas D-T operation reduces the additional heating power required for the transition from those small ELMs to Type I ELMs [9,10] and lower power is required for Type I ELMs at higher plasmas triangularity [19]. Although the power dependence of the ELM frequency of those low amplitude ELMs in plasmas with an ITB has not been studied in detail, we assume they are Type III ELMs on the basis of the similarities in the D_α signature.

The four categories of Type III ELMs (high and low density Type III ELMs, compound ELMs and small ELMs of ITB plasmas) are observed in different regimes (H-modes with and without ITB) and span a very large density range: from very low density $n_e/n_G<0.5$, for ITB plasma, up to densities at, or approaching the Greenwald limit. Given the similarities highlighted before, we compare here the pedestal parameters for those four categories of ELMs. The comparison is shown in Fig.7.

Figure 7 figure shows the pedestal electron temperature T_e, from the ECE heterodyne radiometer, as a function of the electron line average density n_e, given by the outermost channel (R=3.75m, , $\rho\cong0.95$) of the FIR interferometer, for plasmas at 2.5MA/2.4T (the plasmas with ITB have B_t from

2.4 to 2.6T) with low triangularity ($\delta \cong 0.22$-0.25) and strike points on the vertical divertor plates or on the corner of the divertor, near to the throat of the divertor cryopump. T_e is taken at the position of the top of the pedestal. For H-modes with Type I ELMs and for Type III ELMy H-modes at high density, the density profiles are relatively flat, so the density at 3.75m can be taken as the pedestal density. For Type III ELMy H-modes at low density, where the density profile are more peaked (see Section 7), taking n_e at 3.75m may overestimate somewhat the pedestal density. As shown in Fig.7, the Type III ELMs of plasmas with an ITB have the lowest pedestal density and the highest pedestal temperature. In the ELMy H-mode regime, the lowest pedestal density (and highest T_e, $T_e \cong 1600$eV) is achieved for a plasma configuration with the strike points in the corner of the divertor. This configuration is optimised for pumping by the JET divertor cryo-pump. As shown in Fig.7, the corner configuration produces standard H-mode with very low pedestal density and pedestal temperature in the same range as the T_e of plasmas with ITB. Therefore, the pedestal parameters for low density Type III ELMs, which follow the expected inverse power dependence of f_{ELM}, overlap the n_e-T_e operational space of the small ELMs of ITB plasmas, giving confidence to the assumption that the latter are indeed also Type III ELMs. The continuous and dotted arrows in Fig.7 describe the n_e-T_e trajectory of the pedestal top with Type I ELMs that are followed by compound ELMs. The drop in pedestal temperature associated to the Type I ELM crash is followed by the evolution of the pedestal parameters towards lower n_e and higher T_e during the phase of compound ELMs. The compound ELMs can be seen as temporary transitions to the Type III regime from which the confinement is then recovered. Their trajectory in the n_e-T_e space is in the region of intermediate densities and temperature.

At high pedestal density and low temperature, Fig 7 shows the pedestal n_e and T_e for high density ELMy H-modes where the transition to the Type III ELMy regime is induced by external strong gas fuelling.

To further illustrate the behaviour of the pedestal parameters at the transition from Type I to Type III ELMs at low density and the differences between the corner and vertical configurations, Fig 8 shows the time evolution of D_α, the pedestal and core n_e and T_e, core T_i, and the diamagnetic stored energy W_{dia}, for two low density plasma, at the transition from Type I to Type III ELMs.

The red traces belong to an H- mode with a plasma configuration with the strike points in the corner of the divertor, while the black traces are for a plasma with the strike points on the vertical plate of the divertor. The figure shows, for both plasmas, the large drop in both pedestal and core density at the transition from Type I to Type III ELMs. The pedestal (and core) T_e with Type III ELMs is instead equal to the average value during the Type I ELMy phase for the vertical configuration. In the corner configuration (lower pedestal n_e), the pedestal T_e with Type III ELMs can be higher than the maximum T_e reached in the Type I ELM cycle. The core T_i shows a similar time evolution at the transition from Type I to Type III ELMs, and is higher than T_e in those low density plasmas. The figure also shows the large drop in plasma stored energy at the transition to Type III ELMs. Fig.8 also illustrates that with “compound ELMs” the behaviour of the pedestal n_e

and T_e are similar to what observed at the final transition to Type III ELMs, but the drop in density is smaller.

The density dependence of the critical temperature for Type III ELMs is similar to the one of the critical temperature for the L-H transition [8]. The experimental n_e-T_e at the L-H transition is also shown in Fig.7. Experiments with the GB divertor [8] have shown that, below a critical density, the critical temperature for the L-H transition increases with decreasing density. For densities below this critical density the measured P_{L-H} increases (or remains constant) for decreasing density, so that deviations from the L-H threshold power predicted by the scaling are observed.

Considering together all the observation of Type III ELMs summarised in Fig.7, one can see from Fig.9 (where the same data of Fig.7 are plotted in red) that the pedestal plasma temperature, in the Type III ELM regime, does not depend strongly on density at high n_e, and increases with decreasing density at low n_e. For most of the points of Fig.9, the temperature plotted is a "critical temperature", that is, any increase in T_e will produce a transition to Type I ELMs. In fact, for the TypeIII ELMy H-modes in Fig.7 (red circles), it has been experimentally tested that a small step up in power during the Type III ELMy phase does produce a transition to Type I ELMs. For the ITB plasmas, one can see in Fig.6 that there can be various transitions from Type III back to Type I ELMs within the same discharge. The temperature plotted in Fig.7 and 9 for those plasmas is the T_e just before such transitions. In the high density ELMy H-modes, either a step up in power or a decrease in density triggers the transition to Type I ELMs. One could consider also the T_e during compound ELMs to be "critical", since at higher power the compound ELM behaviour disappears.

Figure 9 also show a set of low density Type III ELMy H-mode data for plasmas at Bt=3.4T. This set of data includes the n_e-T_e for compound ELMs. For this higher B_t (and I_p), high density data are not available. The scatter of the data is larger at 3.4T than at lower field. This larger scatter is at least partially due to the fact that, since fewer dedicated experiments were done at 3.4T and hence fewer data are available at this toroidal field, the 3.4T data represent more an existence domain for Type III ELMs in the n_e-T_e space than a critical boundary for T_e. Figure 9 shows that, while the density dependence of the Type III ELMs critical temperature is similar at low and high B_t, T_e is larger at higher toroidal field.

4.2 DEPENDENCE OF THE TYPE I ELM TRANSITION ON PEDESTAL DENSITY

Since the critical temperature for the transition from Type III to Type I ELMs increases at low density in a similar way as does the L-H critical temperature, one could conceive that, below a certain density, P_{TypeI} might also increase. Experimentally, one indeed finds that increasing the density of a low density Type III discharge reduces the power threshold for Type I ELMs. Already in the Mark IIA experiments we observed that with reduced divertor pumping (and no external fuelling), resulting in higher pedestal n_e and lower T_e, it was possible to maintain Type I ELMs at lower power [3].

Figure 10 shows the result of an experiment carried out in the GB divertor to test the dependence

of P_{TypeI} on density at low density. With identical P_{IN}, the discharge with a constant external fuelling of 10^{22} atoms/s is in the Type I ELM regime (marginally, because compound ELMs are observed) while the discharge with no fuelling collapses to the lower confinement, Type III regime. In a similar manner to the reduced divertor pumping, the effect of the external fuelling is to increase both the edge and core n_e and reduce edge and core T_e. The trajectory of the compound ELMs of the plasma with gas fuelling is indicated in Fig.7 by the dotted arrows while the compound ELMs with no gas fuelling are shown, in the same figure, by the continuous arrow. A possible interpretation of the result of this experiment is that, for the lower density plasmas with no external fuelling, a higher temperature (i.e. higher power) is required for the transition from Type III to Type I ELMs since $T \propto 1/n$. In other words, at low density, P_{TypeI} increases as the density decreases. The behaviour of P_{TypeI} and of the L-H threshold power at low density could explain why the decrease in density and consequent increase of the predicted P_{IN}/P_{L-H}, that accompanies the transition to Type III ELMs (as shown in Fig 1 and discussed in the first section), does not lead to the plasma recovering the Type I ELM behaviour. In the density range where the critical temperature for the transition from Type III to Type I ELMs is $\propto 1/n$, an increase in input power as well as an increase in density triggers a transition to the Type I ELMy regime.

5. TYPE III ELMS AT LOW DENSITY: COMPARISON BETWEEN THE MARK IIA AND MARK II GAS BOX DIVERTORS

With the Mark IIA JET divertor [20], extensive experiments were carried out with ELMy H-modes in Deuterium at high plasma current ($3.5MA \leq I_p \leq 5MA$) and low δ ($\delta \cong 0.22$), in preparation for the JET DT experiment [3]. Those experiments highlighted the limits in operational space for Type I ELMy H-modes at low triangularity, when operating at high current and toroidal field. One of the main restrictions for these experiments was the limited additional heating power available in JET: the available power was marginal/not sufficient to achieve H-modes with Type I ELMs at high I_p. In high I_p plasma, a transition to the L-mode regime, sometimes preceded by a brief period to Type III ELMs, was observed [21]. Although the occurrence of the L-mode transition was associated with operation with input powers P_{IN} too close to the H-mode threshold power P_{L-H} [21], this transition occurred at relatively high input powers, up to about twice the L-H predicted threshold power. The correlation between the power required to maintain Type I ELMs and the L-H threshold was confirmed by the D-T experiment, where a wider operational space in Type I ELMs for high I_p plasmas was found, consistently with the inverse isotope mass dependence of the L-H threshold.

Figure 11 shows a comparison between the transition to L-mode observed with the Mark IIA divertor at high I_p and the transition to the Type III ELMy regime with the GB divertor.

Most of the results described in the previous sections are common for ELMy H-modes with the Mark IIA and the Mark II Gas Box divertor, the most significant difference is that with the Mark IIA divertor the plasma was in L-mode for $P_{IN} < P_{TypeI}$. The experiments in Mark IIA and GB used a different plasma magnetic configuration: the divertor strike points were on the horizontal divertor

target in Mark IIA, while with the GB divertor, due to the presence of the divertor septum, only configurations with the strike points on the vertical divertor target, or on the corner of the divertor, were possible (see Fig.12.). The measured H-mode power threshold for GB discharges with the strike points on the vertical target is higher than the H-mode power threshold for Mark IIA plasmas with the strike points on the horizontal target [8 and 18]. Consistently, we find that higher power is required to maintain a Type I ELMy Hmode in steady state in GB than it was required in Mark IIA. In summary, while both the measured P_{L-H} and P_{typeI} were lower with the Mark IIA divertor, a transition from the Type I ELMy regime to L-mode was observed in Mark IIA at $P_{IN}<P_{typeI}$. Those two findings are in apparent contradiction. Most probably, what prevented the Mark IIA plasmas from maintaining an H-mode pedestal with Type III ELMs was the presence of a n=1 MHD instability localised in the pedestal region [21].

This mode was always present during the L-mode phase (but not during the short Type III phases, if they were present), and it disappeared if the plasma made a transition back to Type I ELMs in the same discharge. As reported in [21], the mode had low frequency of the order of hundred Hz. This n=1 mode was localised in the plasma edge, since $m>q_{95}$. In some cases, as the one shown in Fig.13, the mode and the D_α signature were correlated. The nature of this instability as well as the reason why it is not present with the GB divertor is not known. The mode was clearly stable at the power levels required for a steady state H-mode with Type I ELMs. Similar to the ELMy H-mode behaviour, plasma with an ITB also had an L-mode edge with the Mark IIA divertor but an H-mode edge with the GB divertor [22].

6. DISCUSSION AND COMPARISON OF THE EXPERIMENTAL DATA WITH MODELS

As described in Section 3, the pedestal n_e-T_e of Type III ELMy H-modes in JET covers a wide range of density and temperature. At low density, the pedestal T_e increases with decreasing pedestal density approximately as 1/n and increases with increasing toroidal field (see Fig.9). At high density the pedestal temperature is independent of density or the density dependence is very weak. The Type III ELMy data of Fig.9 have been compared with the model proposed by O. Pogutse and Y. Igitkhanov [23,24]. According to this model, Type III ELMs are caused by resistive interchange instability where the driver is provided by magnetic flutter (RIF). When the radial electric field just inside the separatrix becomes sufficiently strong, it can stabilise the RIF. This condition gives the upper boundary for Type III ELMs in the n_e-T_e diagram as:

$$\beta` \lambda`^{-1/3} \rho`^{-1/3} > c_\tau^{\ 2} q^2.$$

Where $\beta=(M_i/m_e)^{3/2}\beta_n s^2/q$ and $\rho`= \rho/R$ is the normalised toroidal Larmor radius. $\lambda`= 1/\nu`$, where $\nu`$ is the dimensionless flutter frequency: $\nu` =c_F s (1+ c_\nu^{\ 2} \{qR/\lambda_e\}^2)^{1/2}$, [23,24].

From this condition, the asymptotic scaling for the critical temperature for the transition from Type III to Type I ELMs can be derived for two ranges of collisionality:

$$T_{0cr} \propto (c_\tau{}^2\, c_F\, c_\nu)^{6/17}\, q^{\,24/17}\, R^{\,4/17}\, B_0{}^{\,10/17} / A^{\,8/17}\, s^{\,12/17} \text{ for } \lambda_e < c_\nu\, q\, R$$

$$T_{0cr} \propto (c_\tau{}^2\, c_F\, c_\nu)^{6/5}\, q^{\,18/5}\, R^{\,-2/5}\, B0^{\,2} / A^{\,8/5}\, s^{\,12/5}\, n_0{}^{\,6/5} \text{ for } \lambda_e > c_\nu\, q\, R$$

Where c_τ c_F and c_n are fitting constants, ne and Te are taken at the top of the H-mode pedestal and the safety factor q and shear s are taken as q_{95} and s_{95}. The model prediction of the critical temperature T_{0cr} is compared with the JET data at B_t=2.4T and B_t=3.4T in Fig. 14 (same set of data as Fig.9). The deuterium plasmas at B_t=2.4 and 3.4T have low shear ($s_{95} \cong 3$) and similar q_{95} (q_{95} from ≅3 to ≅3.3). For both toroidal fields, the data include ELMy H-mode plasmas and plasmas with simultaneous ITB and ETB. The fit coefficients have been adjusted to fit the 2.4T data, and the same coefficients were used then for the 3.4T data and for the analysis presented in the following figures. Although the coefficients used here for the Type III ELMs boundary are different from the ones used in ref [24, see also 25 and 26] to fit the Type III ELM boundary for ASDEX-U, DIII-D and Alcator C-MOD, using the same coefficients given in [24] to fit the JET data, gives little difference in the predicted curves for T_{0cr}.

This analysis shows that there is good agreement between the model and the experimental data. In particular, the model reproduces the strong increase of the critical temperature of Type III ELMs with B_t that is observed at low collisionality.

In Fig 15, the same set of data of Fig 14 is shown with the addition of L-H transition data at 2.4T, already presented in Fig.7. The data for the electron temperature just before the L-H transition (at the position where the top of the H-mode pedestal is observed later in the discharge, when the H mode is fully formed) are fitted to the L-H transition model prediction from [27, 24]. In this model, the condition for the L-H transition is given by the stabilisation of the Alfvén drift wave instability. The coefficients used here for the L-H transition curves are fitted to the JET data, so they are different from the ones given in [27]. The curve for the predicted L-H temperature boundary at 3.4T is also shown in the figure. For the 3.4T data of plasmas with ITB, the predictions of the L-H and Type III models [23,24] are compared, at low collisionality, with the L-mode data (just before the L-H transition) and ELM free data (just after the transition from the Type III to the ELM free regime). The comparison of L-H data with models [see 28] is outside the scope of this paper: the comparison of the models with the L-H and ELM free data is shown here to illustrate that the combination of those two models predicts the narrow density operational space between L-mode, Type III ELMs and Type I ELMs that is found, experimentally, at low collisionality.

While both in ASDEX-Upgrade and in C-MOD the Type III ELMs are found only at high collisionality, Type III ELMs at low density/collisionality were identified also in DIII-D [29]. In DIII-D, the Type III ELMs are found in separated collisionality regions of the n_e-T_e space, i.e. no data are found at intermediate collisionality. As pointed out in section 2, the intermediate collisionality region in the n_e-T_e diagram of the 2.4T JET data is filled by the trajectory of “compound ELMs”.

The absence of steady state Type III ELMs in this region might be due to the specific experimental conditions, since most experiment to study Type III ELMs are carried out either at low density and power, or very high density. Still, the DIII-D observation could suggest that different physics

mechanisms could be responsible for Type III ELMs at low and high collisionality. From the comparison of the characteristics of the Type III to Type I transition in standard ELMy H-modes and plasmas with an ITB, current driven peeling modes are indicated in [1] as the candidate instability causing Type III ELMs at low collisionality. Type III ELMs are observed in ITB plasmas at much higher input power than the power required to maintain Type I ELMs in standard ELMy H-modes [1 and 17]. According to [1], there are strong indications that the main difference between plasmas with and without ITB could be due to the different current profile and, in particular, to the larger fraction of edge current in ITB plasmas preventing the transition to Type I ELMs. Current driven peeling modes are then stabilised by the increased pressure gradient at higher power [30]. Although the results from [1] might also suggest a different physics mechanism for Type III ELMs in ELMy H-modes and plasmas with ITB, experiments where the plasma current was ramped down in low collisionality standard Type III ELMy H-modes demonstrate that the edge current might determine the Type I/III ELM transition also in this regime. In Fig 16 the time traces with two low density ELMy H-modes without I_p ramp are compared with identical plasmas with an I_p ramp down from 2.5 to 2MA during the Type III ELMy phase (with P_{IN} just below P_{TypeI}). Fig.16 shows that, in the discharges where the plasma current was ramped down, a transition from Type III to Type I ELMs was observed. At the transition to Type III ELMs, the local n_e-T_e are consistent with the prediction of the model based on resistive interchange instability. Although the short delay (<100ms), between the start of the I_p ramp and the changes in pedestal and ELM behaviour, suggests an effect only in the plasma edge, an immediate reduction of transport is seen also in the plasma core (Fig.17). Experiments where the plasma current was ramped up in an H-mode with Type I ELMs in order to trigger a transition to Type III ELMs did not produce any change in ELM behaviour. This phenomenon might be due to the fact that in those plasma the additional heating power was much larger than P_{TypeI}. In fact, this result is in contrast with another experiment carried out with the Mark IIA divertor, where an I_p ramp down produced a transition to L-mode (see section 5), and I_p ramp up was observed, inversely, to produce a transition from an L-mode to an H-mode with Type I ELMs [21].

The results of the I_p ramp experiments suggests that it is likely that low density Type III ELMs for plasmas with and without ITB are driven by the same instability. In addition, as pointed out in Section 3, standard ELMy H-modes can have pedestal n_e and T_e in the same region of the pedestal n_e-T_e operational space for ITB plasmas, and therefore similar pedestal collisionality. Moreover, the same pedestal temperature boundary at B_t=2.4 and 3.4T seems to define well the transition from Type III ELMs to Type I ELMs both for plasmas with ITB [see also 10, 31] and without ITB. The changes observed with plasma triangularity are also similar: in both scenarios, lower power is required for the transition from Type III to Type I ELMs at higher plasmas triangularity [19]. Finally, also common to the two regimes is the observation that D-T operation reduces the additional heating power required for the transition to Type I ELMs [9,10], indicating an inverse mass dependence of P_{TypeI}, and the different behaviour of the Mark IIA (L-mode edge) and GB divertor (H-mode edge)[22].

At high density, result from JET and ASDEX-U, C-MOD and DIII-D, show that the transition from Type I to Type III ELMs happens above a critical temperature, which is independent of density and increase weakly with toroidal field [24].

In Fig. 18, the predicted boundary [23,24] between Type I and Type III ELMs at high density is shown for the density scans at 8, 11 and 14MW of input power described in Section 7. The L-H predicted boundary [27] is also plotted in the figure, to show that the majority of the data for Type III ELMs are found above the predicted L-H boundary.

The JET data suggests that, at high collisionality, the critical temperature for Type III ELMs does not depend strongly on triangularity (see Section 7), consistent with the model prediction. In fact, according to the Pogutse and Igithkanov model, the shear dependence of T_{0cr} should be stronger at low collisionality. The variation in the edge shear of the JET low density ELMy H-modes with Type III ELMs is too small to verify the predicted shear dependence of T_{0cr}, but the variation in critical temperature is consistently small both in the model predictions and in the few data available. Note that the decrease of P_{TypeI}, observed in high triangularity ELMy H-modes both at low and high density, could also be related to the physics mechanism governing the low pressure boundary of the Type I ELMs [32], i.e to different the crash of temperature and density at the ELM event.

The mass dependence predicted by the Pogutse Igithkanov model was checked against the JET data. The comparison of the data for different isotopes is carried out using the temperature from LIDAR, since the ECE data were not available for the hydrogen plasmas. The LIDAR T_e data are taken at a fixed position, (R=3.75m), which is further inside the plasma compared to the typical position of the pedestal. Since the temperature profile are not as flat as the density profiles, the absolute value of the T_e given by LIDAR at 3.75m, is generally higher than the pedestal temperature, so that the data cannot accurately be compared with the model predictions, since the fitting coefficient for the model were derived by fitting T_e data from ECE. Even if a quantitative comparison is not possible, Fig.19 shows nevertheless that the high density Type III data for different isotopes seems to be separated in density more than in temperature and that the model does not reproduce the trend observed in the experimental data.

Finally, as shown in Fig.20, the model of Pogutse-Igithkanov predicts a too strong dependence of the critical temperature on q_{95} for high density ELMy H-modes. This wrong dependence of the predicted boundary on q_{95} was also reported, at low collisionality, for plasmas with ITB [31].

A different model for Type III ELMs at high collisionality correctly describes the q_{95} dependence observed in JET for the transition from Type I to Type III ELMs at high density. According to the Chankin and Saibene model [33], Type III ELMs at high density are driven by resistive ballooning instability, and the dimensionless pressure gradient, $F=q^2R\Delta\beta/f(s)$ (pressure gradient normalised to the ballooning limit), and collisionality $\nu^*_e=Z_{eff}n_eqR/T_e^2$, are the key parameters responsible for the threshold of both ideal and resistive ballooning instability. At the transition from Type I to Type III ELMs, while the pedestal temperature (and pressure) always decreases, the pedestal density might either increase or decrease (see also Section 7). If the fuelling is increased further with

Type III ELMs, an H-L transition is eventually observed. As a consequence, there is a limiting value for the maximum density achievable in an ELMy H-mode. This critical density is given either by the maximum density achievable with Type I ELMs (critical density for the transition to Type III ELMs) or by the density prior to the HL transition. The H-mode limiting density is usually expressed in terms of the Greenwald density limit, or similar expressions of the form $\beta^{\alpha}/q^{\beta}R^{\gamma}$. A scaling of the critical density for the transition to Type III ELMs of this form is derived in [33] by fixing the two dimensionless similar parameters F and ν^*. Experimentally, the density at which the transition from Type I to Type III ELMs is observed in JET is found to scale, at high density, as $n_{e,crit}=B_t/q^{5/4}$. This dependence agrees with the prediction from the model: $n_{e,crit} \sim B_t f(s)^{1/2}/q^{5/4} R^{3/4} Z_{eff}^{1/4}$. This is shown in Fig. 21, where n_{ped} data at the transition to high density Type III ELMs are plotted with the scaling curve. The data in the figure are from ref. [11] and from I_p-B_t scans in high density ELMy H-modes with Type III ELMs, at constant plasma shape, P_{IN} and s_{95}.

In summary, the critical temperature for the stabilisation of Type III ELMs, predicted by the model of Pogutse and Igithkanov is in good agreement with both the B_t and density dependence of the JET deuterium data at constant q_{95}. Moreover, this model describes well, with a single set of fitting coefficients, the data from different Tokamaks. This suggests that the model predicts the correct form of the scaling of T_{crit} in the β ρ ν variables.

As noted before, the combination of this model with the L-H transition model predicts the relatively narrow density operational space between L-mode and Type I ELMs, which is observed experimentally in plasmas with ITB at low collisionality. According to these models, the widest operational space with Type III ELMs (in particular at low collisionality) should be achieved with low magnetic shear and high B_t (as is the case for the ITBs plasmas analysed in this paper). In contrast, due to the I_p dependence of the predicted $T_{crit,\ L\text{-}H}$, high plasma current and high shear should move the L-mode boundary to higher densities and reduce the Type III ELM region, to the extent that the H-mode transition could be directly in the ELM free regime. On the other hand, JET experiments have shown that $T_{crit,\ L\text{-}H}$ does not depend on plasma current, [8].

Discrepancies between Pogutse-Igithkanov model and experimental data are found regarding the dependence of T_{0crit} on isotopic mass and q. The Chankin- Saibene model predicts the critical density for the transition to Type III ELMs at high collisionality, and the predicted inverse q_{95} dependence is in good agreement with the experimental data. It is difficult, given their different nature, to make a direct comparison between the two models. It is possible, however, that resistive ballooning and interchange instability are combined at high density, where the gap between the ideal ballooning and L-H transition in the n_e-T_e diagram narrows. At low collisionality, the behaviour with I_p ramps and the analysis of ITB plasmas [1] suggest peeling modes as the instability triggering Type III ELMs.

Although it is possible that a different instability is responsible for high and low collisionality Type III ELMs, the JET data also shows a continuum in the n_e-T_e operational space which includes data at intermediate collisionality. Moreover, there are common experimental observation for both

low and high collisionality Type III ELMs such as the ELM frequency variation with power, the occurrence of those ELMs at low power above the L-H threshold, the variation of P_{TypeI} with plasma triangularity as well as the quantitatively similar degradation of H factor, compared to the Type I ELMs at the same density (see next section).

5. ENERGY CONFINEMENT OF TYPE III ELMY H-MODES

In JET ELMy H-modes with Type III ELMs, the energy confinement enhancement factor relative to Hmode scaling (H98(y,2),[34]) is lower than for Type I ELMs, over the entire density range. This is illustrated in Fig.22, where the H factor is plotted against the fraction of the core line averaged density over the Greenwald density, for Type I and Type III ELMs. Figure 11 also shows that H factor of Type III ELMy H-modes degrades with density in a similar way as for Type I ELMy H-modes [11]. The observation that Type III ELMy H-modes with increased triangularity can achieve higher density with better confinement (see Fig.23, from [14], and [35]) is also similar to the Type I ELMy H-modes behaviour. Although data of the energy confinement dependence on triangularity are scarcer for Type III ELMs than for Type I ELMs, the trend shown in Fig.23 is confirmed by the data in the JET ELMy H-mode steady state database and holds over the entire density range. As reported in [11], in high density Type III ELMy H-modes, the degradation of confinement (compared to Type I ELMs) is characterised by enhanced edge cooling and reduced pressure gradient. At the transition, the decrease of pedestal temperature at the transition is not compensated by any increase in the pedestal density resulting in a net loss of pedestal pressure.

The pedestal n_e and T_e at the transition from the Type I to the Type III ELMy regime at high density are shown in Fig.24 for 2.5MA/2.7T plasmas at different triangularity: $\delta\cong 0.23$ (black symbols), $\delta\cong 0.38$(red symbols) and $\delta\cong 0.47$(blue symbols). The density scans at $\delta\cong 0.23$ (with 11MW NBI), $\delta\cong 0.38$ and $\delta\cong 0.47$ are the same density scans shown in Fig.23. In addition, the data from two further density scans with $\delta\cong 0.23$ with 8 and 14MW NBI are included in Fig.24. In this figure, the full symbols represent the n_e-T_e data for the top of the H-mode pedestal in Type I ELMy plasmas (average over the ELM cycle) and the empty symbols are the pedestal data for the Type III ELMy plasmas. The dotted line in the figure divides the Type I ELMy regime from the Type III ELMy regime in terms of pedestal temperature, and indicates that, at least at high density, the critical temperature for the transition to Type III ELMs does not seem to depend on triangularity. Fig.24 also shows that, as the gas fuelling is increased in subsequent discharges with Type III ELMs, the pedestal temperature (and the global confinement, see Fig.23) of the Type III ELMy plasmas decreases, as indicated by the arrows in Fig.24. While the pedestal T_e always decreases as the fuelling is increased in plasmas with Type III ELMs, the pedestal density responds by either increasing or decreasing. At least for low triangularity plasma, where the degradation of confinement with density in the Type I ELMy regime is more pronounced than at high δ, the pedestal pressure degrades continuously from the Type I to Type III ELMy regimes, with the Type I ELMy plasmas at the highest density and the Type III ELMy plasmas having very similar pedestal pressure and confinement.

The plasma with $\delta \cong 0.47$ in Fig.24 has a different behaviour than those at lower δ at the transition from Type I to Type III ELMs: a large decrease of the pedestal n_e is observed as well as the drop of the pedestal T_e. It is not clear what causes this loss of pedestal n_e, or if the correlation between the different behaviour of the pedestal ne at the transition to Type III ELMs and the plasma δ, that is suggested by the data in Fig.24, is indeed an effect of triangularity. In fact, a decrease in pedestal density at the transition to Type III ELMs is sometimes observed also at low δ (see also ref [11]). As reported in [11], the observed decrease in pedestal stored energy at the transition to Type III ELMs at high density does not totally account for the global confinement losses and increased core transport also plays a role.

In low density ELMy H-modes, the lower plasma pressure is not due to the cooling of the pedestal, as at high density, but to lower density (compared with Type I ELMs) across the plasma profile. The central beam fuelling at low edge ne produces slightly more peaked density profiles with Type III ELMs than with Type I ELMs. The central and pedestal Te are either unchanged or increased with Type III ELMs compared to Type I ELMs, and $T_i > T_e$. Both the T_e and T_i profiles are more peaked during the low density Type III ELMs than with Type I ELMs.

SUMMARY AND CONCLUSIONS.

The Type III ELMy regime in JET is found in a large operational space in terms of the pedestal n_e-T_e, with Type III ELMs being observed in standard ELMy H-modes as well as in plasmas with an internal transport barrier. Steady state Type I ELMy H-modes are only observed above a critical power, $P_{TypeI.}$. At powers just below P_{TypeI}, the plasma can access the Type I ELM regime and sometimes maintain it for several energy confinement times, but cyclic or permanent transitions to Type III ELMs are then observed. In JET, for a given plasma triangularity, P_{TypeI} is proportional to the L-H threshold power and decreases for increasing δ. P_{TypeI} is also observed to increase at low density. The highest P_{TypeI} is for low density low triangularity ($\delta \cong 0.25$) plasma where the Type I ELMy regime and the good confinement associated with it can be maintained in steady state with a power of about twice the L-H threshold power. A reduction of P_{TypeI} of 20-30% is observed for an increase in δ from $\delta \cong 0.2$ to $\delta \cong 0.3$.

In the pedestal n_e-T_e diagram, the density of JET plasma with Type III ELMs can be as low as 20% of the Greenwald limit n_G, or as high as $\cong n_G$. The critical pedestal temperature for the transition to from Type III to Type I ELMs, Tcr, increases with decreasing density ($T_e \propto 1/n_e$) at low density, and is approximately constant at high density. At low density, T_{cr} increases with toroidal field ($T_e \propto B_t^2$) at constant q_{95}.

Plasma with an ITB and Type III ELMy edge have generally lower pedestal n_e and higher pedestal T_e than standard ELMy H-modes. Nevertheless, with a similar plasma configuration optimised for divertor pumping, the n_e-T_e of low density Type III ELMy H-modes overlaps with the operational range of plasmas with an ITB. Similar to what is observed in standard ELMy H modes, an increase in density at constant power can trigger a transition to Type I ELMs also in Type

III ELMy plasmas with ITB [10]. Also similar for the two regimes is the observed reduction of the power required to access the Type I ELMy regime with increasing triangularity [19] and isotopic mass. The similarities in the pedestal behaviour of plasmas with and without an ITB indicate that the ELMs are driven by the same instability, despite the fact that only for standard ELMy H-modes has it been proven in JET that the ELM frequency follows the inverse power dependence, typical of Type III ELMs. The most significant difference between the two regimes is the much higher power at which Type III ELMs are still observed in plasma with ITB. This difference cannot be explained only in terms of the decrease of PTypeI with decreasing density [1]. All the above results are common to the JET Mark IIA and GB divertors. Only one significant difference between the two divertor was observed in low collisionality plasma with and without ITB: at powers below P_{TypeI}, the Mark IIA plasma remained in L-mode. This difference is attributed to the presence of an additional n=1 low frequency pedestal instability in the MARK IIA plasmas, which prevented them from maintaining an H-mode pedestal with Type III ELMs. This instability, of unknown nature, was stabilised for $P>P_{TypeI}$.

The JET data, in contrast with results from other tokamaks, indicates that the operational space for Type III ELMs covers a wide range of pedestal collisionality. The common observations at low and high collisionality are the ELM frequency dependence on power, the occurrence of Type III ELMs at low power above the L-H threshold power, the effect of plasma triangularity and isotopic mass and, not discussed in this paper, the fact that, the ELM crash is smaller than for Type I ELMs in the entire collisionality range [35]. Those common observations are indicative of a common physics mechanism for the ELM trigger.

A model for Type III ELMs (Pogutse-Igithkanov, [23, 24]), which consider the resistive interchange instability with magnetic flutter, was tested against the JET experimental data. The model predicts well, over the entire collisionality range, the density dependence of the critical temperature for the transition to Type I ELMs in JET as well as in other tokamaks (with a single set of fitting parameters). In JET, this model also predicts the experimentally observed toroidal field dependence of the critical temperature of Type III ELMs. Nevertheless, such model does not correctly describe the experimental variation of the critical temperature with isotopic mass and with q_{95}. Other experimental observations suggest instead that a different instability might be responsible for Type III ELMs at different collisionality. At low collisionality, in plasmas with and without an ITB, a current ramp down triggers the transition from Type III to Type I ELMs, indicating a role of the edge currents and suggesting current driven peeling modes as candidate instability. At high collisionality, a model (Chankin-Saibene, [33]) based on the resistive ballooning instability correctly reproduces the JET data for the transition from Type I to Type III ELMs in terms of critical density : $n_{e,\,crit} = B_t/q^{5/4}$.

In JET Type III ELMy H-modes, the energy confinement enhancement factor degrades with density and increases with triangularity over the entire collisionality range in a similar way as for H-modes with Type I ELMs, indicating that those two trends are not specifically related to the

ELM type. Although the reduction of confinement with Type III ELMs with respect to Type I ELMy H-modes is quantitatively similar at high and low density, the signatures are different. In fact, while at high density the degradation of confinement is mainly due to the cooling of the pedestal (sometimes accompanied by loss of pedestal density), at low density the pedestal temperature does not vary or increases at the transition to from Type I to Type III ELMs, and the loss of pedestal pressure is mainly caused by a strong decrease of the pedestal density. Similar to what observed with Type I ELMs, higher density with better global confinement is achieved also in the Type III ELMy regime by increasing the plasmatriangularity. Nevertheless, the few data available suggest that, at least at high density, the relative degradation of confinement at the transition from Type I to Type III ELMs might be more substantial at higher δ, mainly due to the larger loss of pedestal density at the transition.

ACKNOWLEDGMENTS

The authors would like to acknowledge the contribution of the JET Joint Undertaking JET Team to the work presented in this paper.

REFERENCES

[1]. Y. Sarazin, M.Becoulet et al., 2002 Plasma Phys. Control. Fusion 44, 2445
[2]. D.J Campbell, 2001, Phys. Plasma 8, 2041
[3]. L.D Horton, R. Sartori et al, 1999, Nuclear Fusion–**39,** 993
[4]. ITER Confinement Database and Modelling Expert Group (presented by T Takizuka) 1996 Fusion Energy vol II p 795 IAEA-CN64/F-5
[5]. E.J. Doyle et al, 1991, Phys Fluids B, 3
[6]. H. Zohm, 1996, Plasma Phys. Control. Fusion 38, 105
[7]. R. Sartori et al, 1999 Proc 26th EPS on Controlled Fusion and Plasma Physic vol 23J (Geneva, EPS), 197
[8]. L.D. Horton et al, 1999 Proc 26th EPS on Controlled Fusion and Plasma Physic vol 23J (Geneva, EPS), 193
[9]. E. Righi, D V Bartlett, J P Christiansen et al., 1999 Nuclear Fusion 39, 309
[10]. JET Team (prepared by ACC Sips), 2001, Nuclear Fusion 41**,** 1559
[11]. G. Saibene, L D Horton, R Sartori et al, 1999, Nuclear Fusion 39, 1133
[12]. R. Sartori et al, in JET report R(00) 01
[13]. R. Sartori et al, 2002, Plasma Phys. Control. Fusion 44, 1801
[14. G. Saibene, R. Sartori, A Loarte et al, 2002, Plasma Phys. Control. Fusion 44, 1769
[15]. W. Suttrop, M. Kaufmann at al, 1997, Plasma Phys. Control. Fusion 39, 2051
[16]. F.X. Soeldner et al, 1997, Plasma Phys. Control. Fusion 39, B 353
[17]. M. Becoulet et al, 2002 Plasma Phys. Control. Fusion 44, A103
[18]. The JET Team, presented by E Righi, 2000, Proc. 18th Int. Conf. Sorrento, IAEA-CN-77

[19]. P.J. Lomas et al, Proc, 9th European Fusion Physics Workshop, Saariselka, Finland, Dec.2001
[20]. L.D. Horton et al, 1999, Nuclear Fusion **39,** 1
[21]. R. Sartori et al., 1998, Plasma Phys. Control. Fusion 40, 757
[22]. C. Gormezano et al, 1999, Plasma Phys. Control. Fusion 41, 367
[23]. O. Pogutse, Igitkhanov Yu et al., Proc. 26th EPS on Controlled Fusion and Plasma Physics vol 23J p 249
[24]. Yu. Igitkhanov, Pogutse O, 2000, Contrib. Plasma Physics 40, 368
[25]. W. Suttrop, 1999 Plasma Phys. Control. Fusion 42, A1
[26]. L.D. Horton et al., 1999 Plasma Phys. Control. Fusion 41, B329
[27]. O. Pogutse, Igitkhanov, 1997 Proc. 24th Eur. Conf. Berchtesgaden, vol 21A part III, 1041 Page 34.
[28]. The ITER H-mode threshold database working group, presented by E Righi, 1998 Plasma Phys. Control. Fusion 40, 857
[29]. T.H. Osborne et al., 1997 Proc 24th EPS on Controlled Fusion and Plasma Physic vol 21A, part III, p 1101 (Geneva, EPS)
[30]. P.B. Snyder, H R Wilson et al, 2002 Pyisics of Plasma 9, p2037
[31]. M. Becoulet et al, 2001 Proc. 28th Eur. Conf. Funchal, vol 25A, 1605
[32]. A. Loarte et al., 2002 Plasma Phys. Control. Fusion 44, 1815
[33]. A. Chankin and G. Saibene, 1999, Plasma Phys. Control. Fusion 41, 913
[34]. J.G. Cordey et al, Plasma Phys.Control. Fusion 39 (1997), B115
[35]. J. Rapp et al, 2002, Plasma Phys. Control. Fusion 44, 639

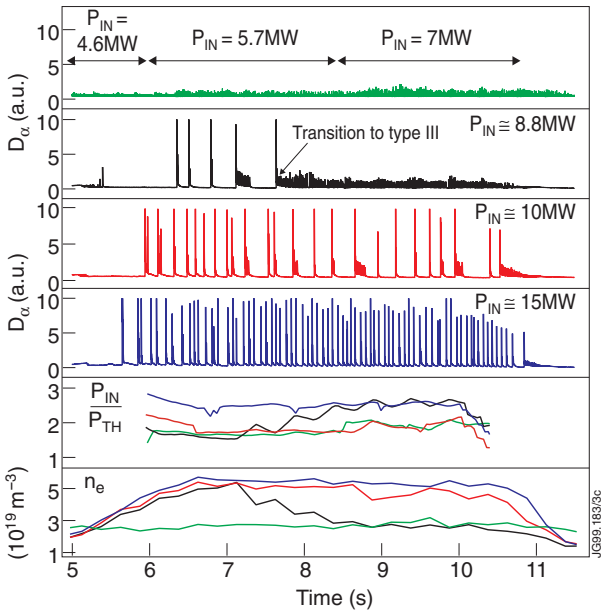

Figure 1: Power scan at 2.5MA/2.5T for a low δ plasma, δ≅0.22,with the strike points on the vertical plate of the divertor. The first four boxes show the time evolution of the D_α signal, for discharges with increasing input power. The last two boxes show the evolution of the ratio of the input power over the predicted L-H threshold power P_{IN}/ P_{L-H}, and of the line averaged density n_e, as the power is increased (Pulse No: 45526,46228,46227,47541)

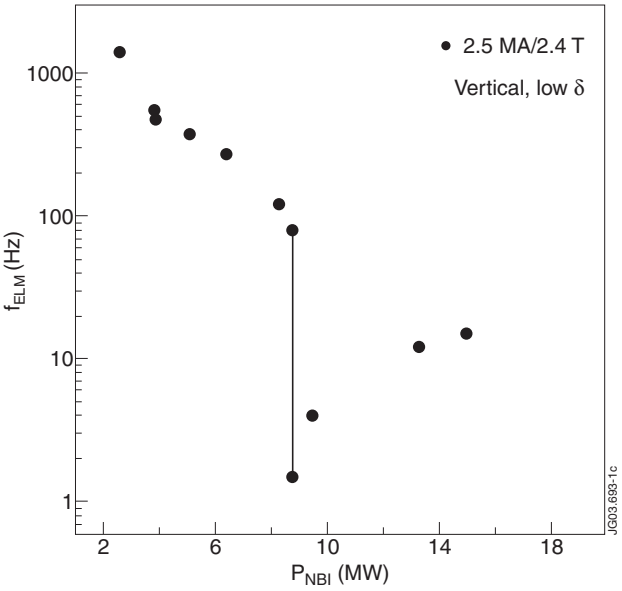

Figure 2: Power scan at 2.5MA/2.5T: ELM frequency versus power. The ELM frequency decreases with increasing NBI power for Type III ELMs and it increases with power for Type I ELMs. T he p lasma with a transition from Type I to Type III ELMs are characterised by a double value of f_{ELM}.

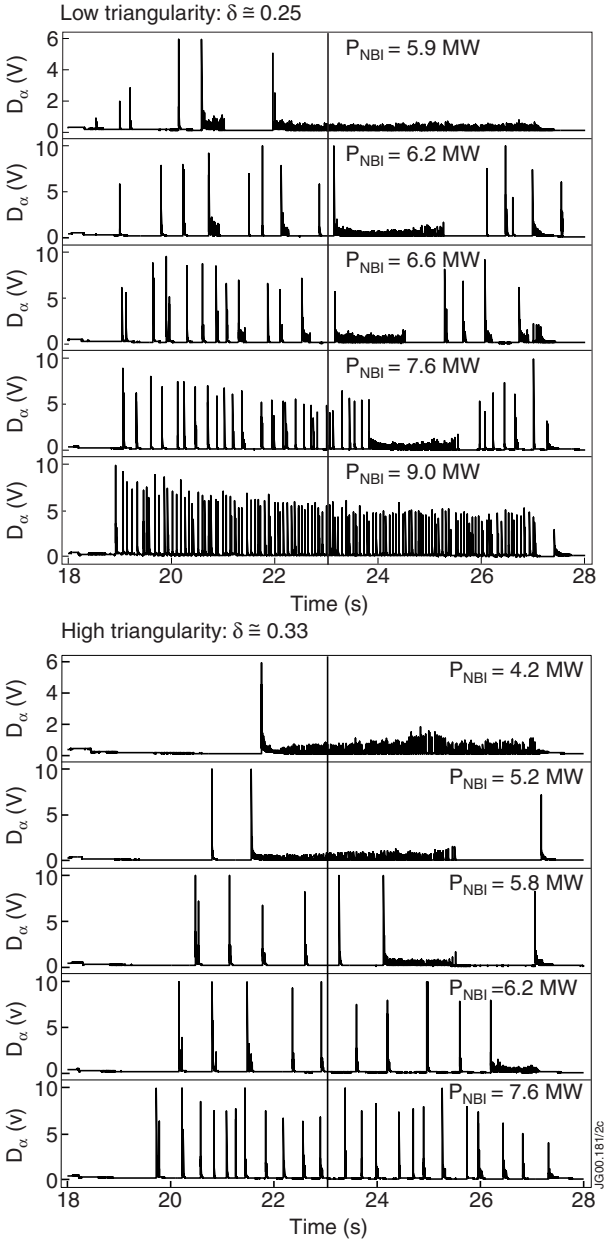

Figure 3: Divertor D_α traces for a power scan at 2.0MA/ 2.0T for a low triangularity plasma, upper figure, and high triangularity plasmas, lower figure (both with the strike points on the vertical divertor target). The vertical line marks a 5s additional heating duration.Note that the duration of the initial phase with Type I ELMs increases with increasing P_{IN}.

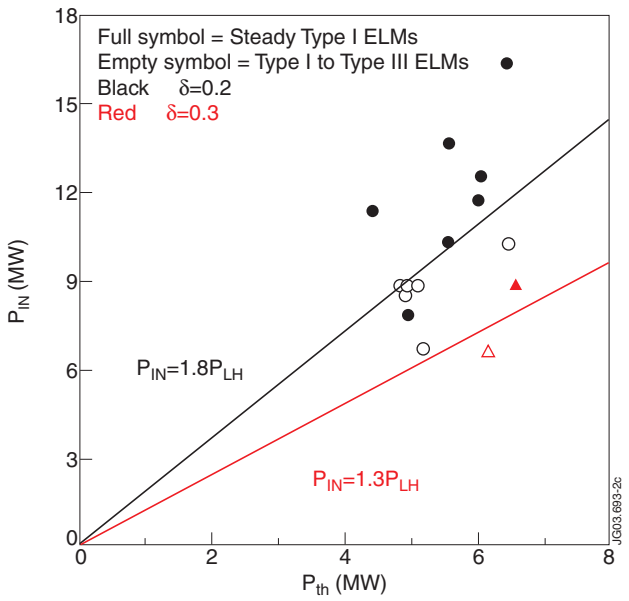

Figure 4: Power required to maintain Type I ELMs in steady state, derived from a P_{IN}, B_t and I_p scan with the JET GB divertor. Full symbols: steady H-modes with Type I ELM, Empty symbols: H-modes with a transition from the Type I to the Type III regime.

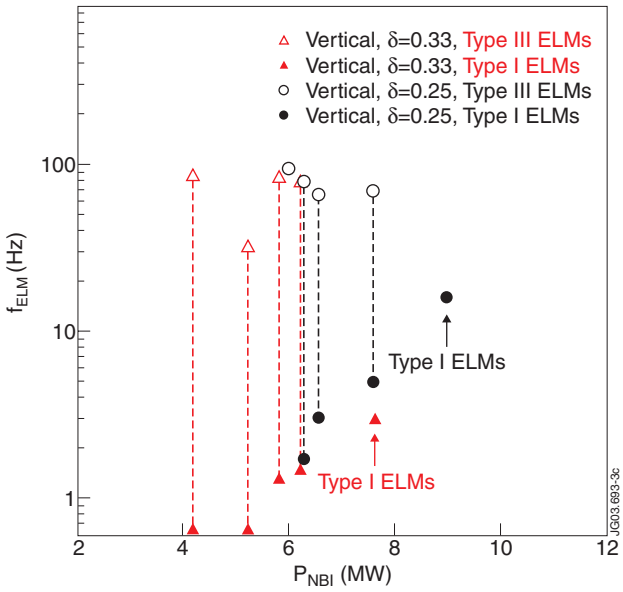

Figure 5:ELM frequency versus NBI power for the power scans at low δ and at high δ of Fig.3. The Type I ELM frequency for the two high δ plasma at the lowest powers is only indicative due to the irregular ELm behaviour at low power.

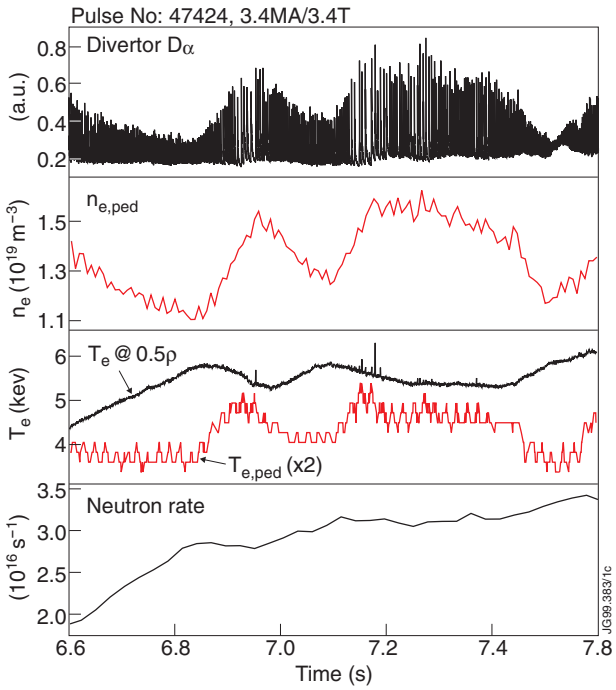

Figure 6: Time traces of divertor D_α, pedestal density, T_e at midradius (inside ITB) and at the pedestal, and neutron production rate, for Pulse No: 47424, with ITB and ETB.

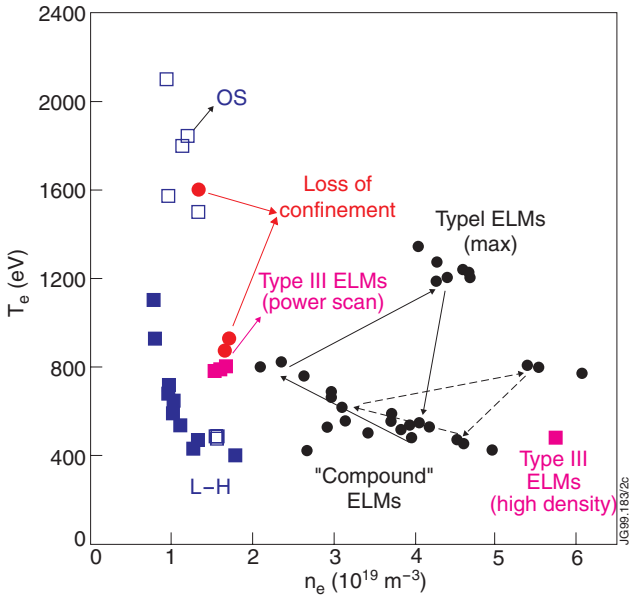

Figure 7: Pedestal n_e-T_e diagram for low triangularity plasmas at 2.5MA/2.4T [7] (the plasmas with ITB, have Bt from 2.4 to 2.6T. The arrows indicate the ELM cycle for a Type I ELM crash followed by compound ELMs.)

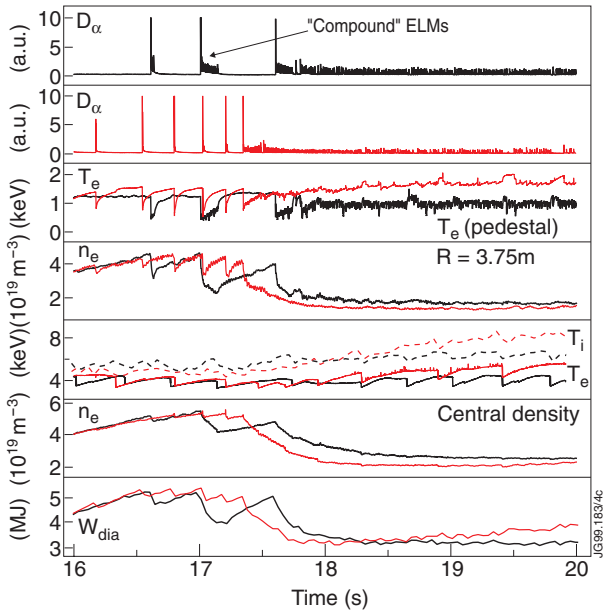

Figure 8:Evolution of the pedestal and core n and Te at the transition from the Type I to the Type III ELMs regimes at low density. 2.5MA/2.4T, P_{IN} = 9MW. Pulse No: 46246 (black): strike points on the vertical target, Pulse No: 46241(red): strike points in the corner

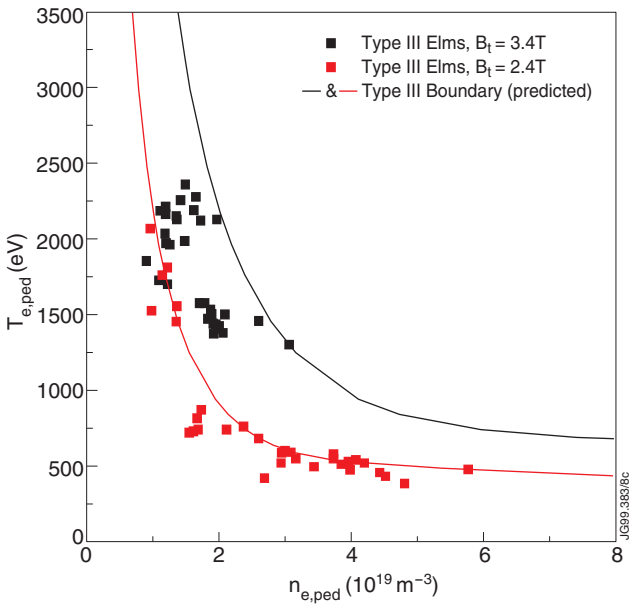

Figure 9: Pedestal n_e-T_e diagram for 2.5MA/2.4-2.6T and 3.3-3.6MA/3.4T Type III ELMy H-modes. n_e from the FIR interferometer outermost channel and T_e from the ECE heterodyne radiometer.

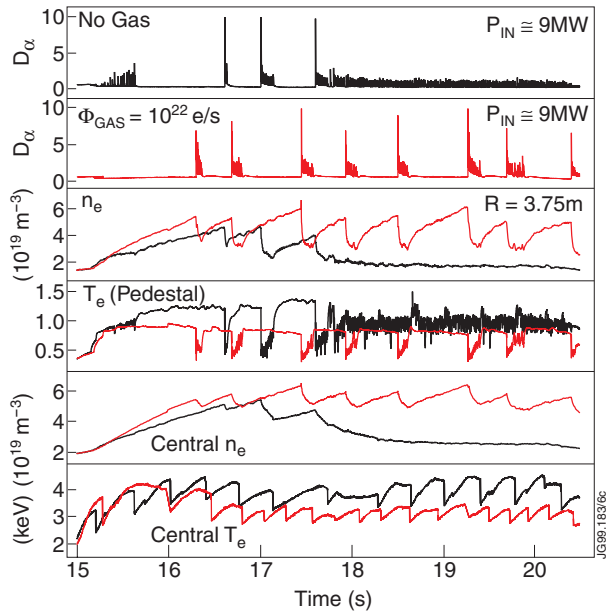

Figure 10: Effect of gas puff. 2.5MA/2.4T, P_{IN} = 9MW Pulse No: 46246: no gas, Pulse No: 46248: with gas fuelling. The pedestal density is given by the outermost channel of the FIR interferometer (see comments on page 11).

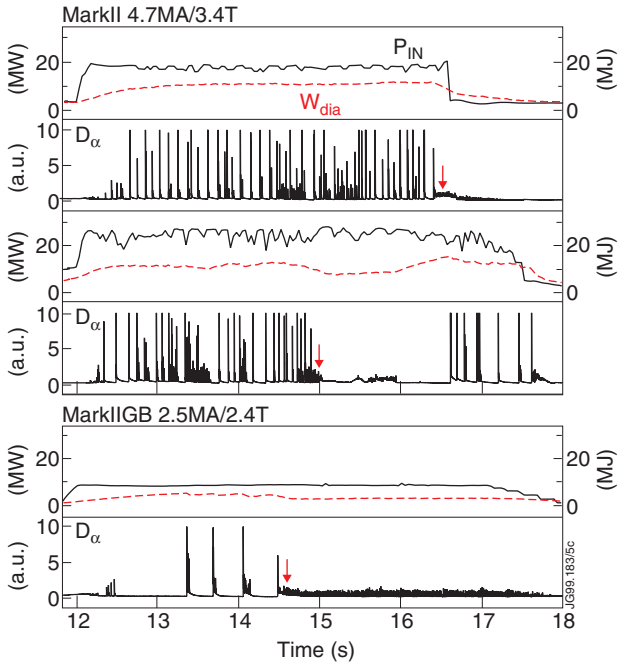

Figure 11: The loss of confinement with the Mark IIA and GB divertors.#38880/38891 at 4.7MA/3.4T (Mark IIA) and 46229 at 2.5MA/2.4T (GB).

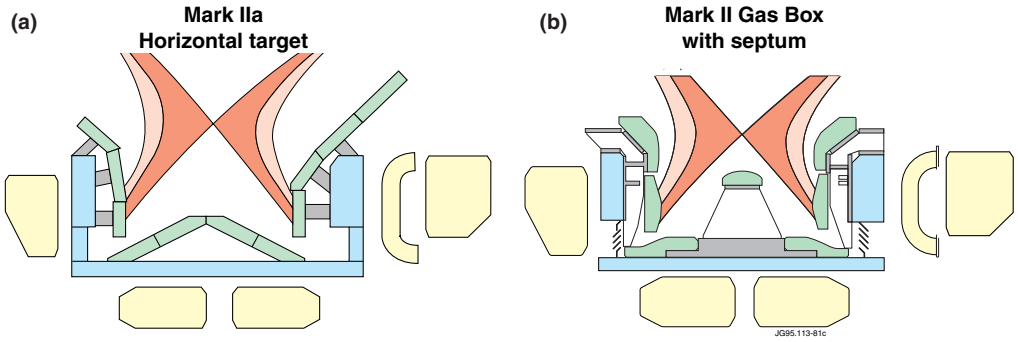

Figure 12: The Mark IIA divertor left) and the GB divertor (right). With the Mark IIA divertor, plasma configuration with the stike points on the horizontal (as in the figure) and vertical target were possible. With the GB divertor, only configuration with the strike points on the vertical target or on the corner of the divertor are possible.

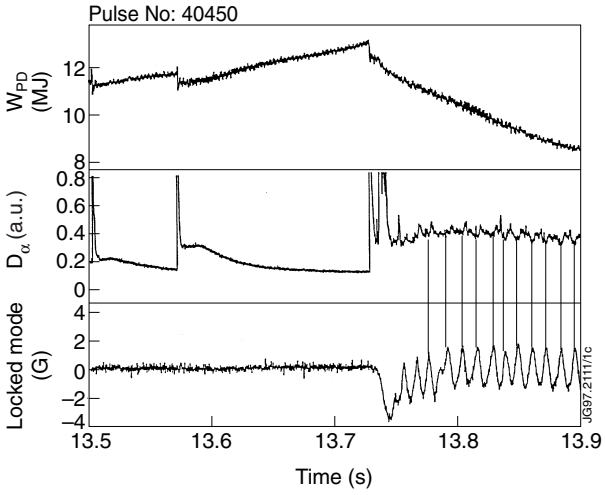

Figure 13: The n=1 mode signature as seen by the locked mode detector and D_α signal

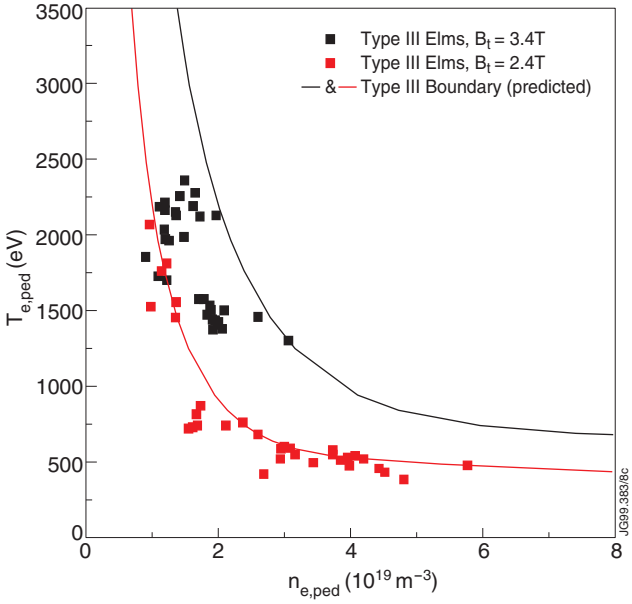

Figure 14: Pedestal n_e-T_e diagram for 2.5MA/2.4-2.6T and 3.3-3.6MA/3.4T discharges. n_e from the FIR interferometer outermost channel and T_e from the ECE heterodyne radiometer .The data are compared with the critical temperature (or upper boundary) for Type III ELMs predicted by the model of [23]and [24].

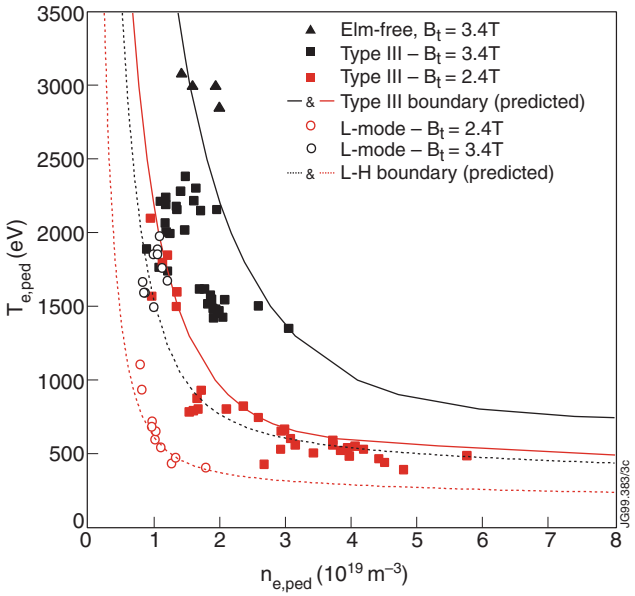

Figure 15: In addition to the set of data of Fig.17 and to the predicted T_{0cr} for Type III ELMs, this figure shows the predicted L-H boundaries for 2.4 and 3.4T plasmas as well as L-H transition data (circles) and data just after the transition from Type III ELMs to ELM free in plasmas with ITB (triangles).

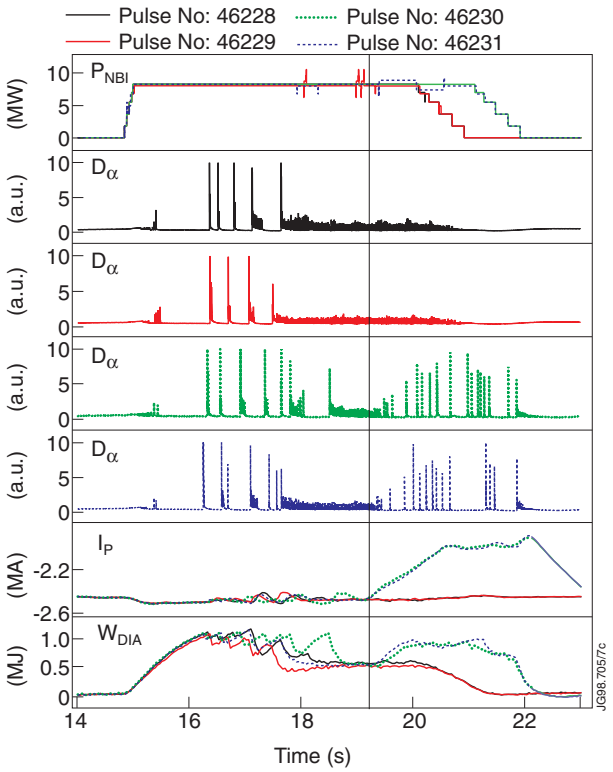

Figure 16: Time traces of the divertor D_a, plasma current and stored energy for ELMy H-modes with (green and blue traces) and without (black and red traces) I_p ramp down. In plasmas with input power just below the power required for steady state Type I ELMs, I_p was ramped down during the Type III ELMy phase. The result of the I_p ramp was a transition from Type I II to Type I ELMs.

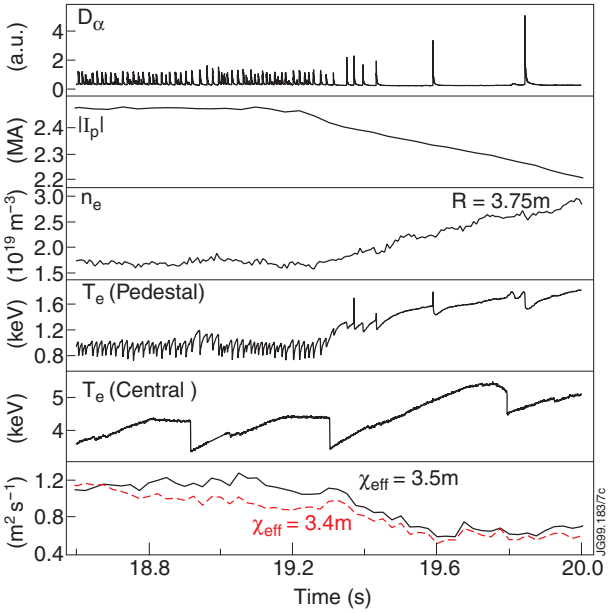

Figure 17: At the transition from Type III to type I ELMs triggered by the I_p ramp down both pedestal density and temperature increase. The increase of the pedestal temperature seen at each sawtooth crash is transient and not sufficient to provoke a transition to Type I ELMs, in absence of the I_p ramp. At the transition, the transport is reduced also in the plasma core.

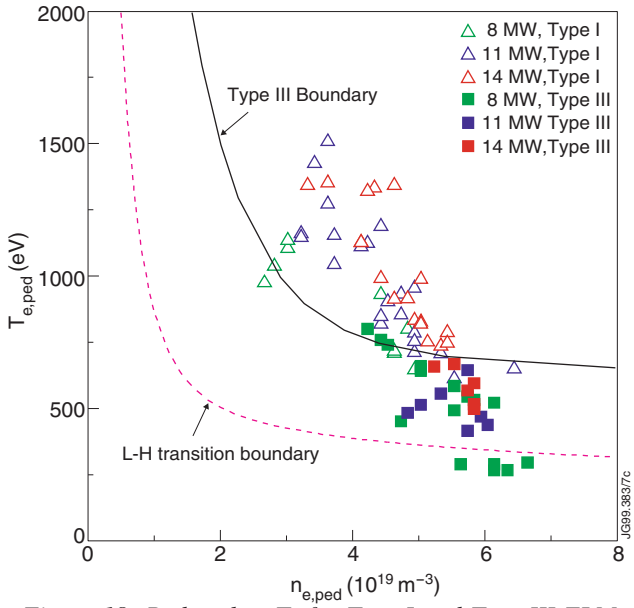

Figure 18: Pedestal n_e-T_e for Type I and Type III ELMs from Mark IIA discharges at 2.5MA/2.7T. A density scan was carried out for each level of P_{IN} (8-11 and 14MW NBI).

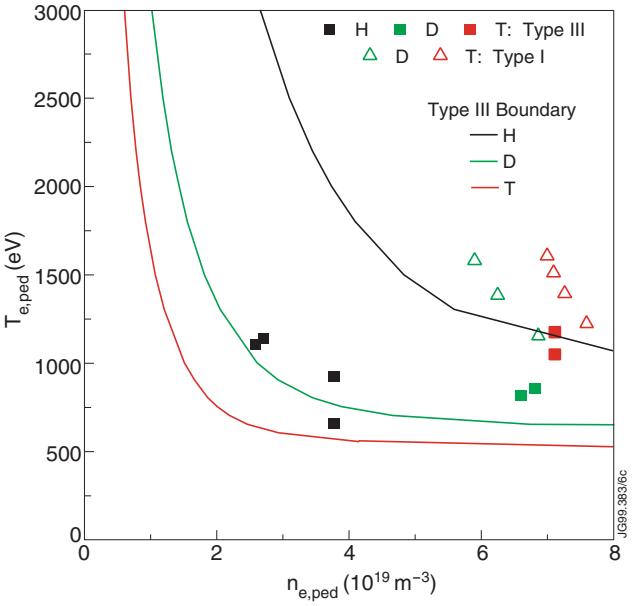

Figure 19: Pedestal n_e-T_e (LIDAR data @3.75m radius) for gas scans in H, D and T at 2.5MA/2.7T.

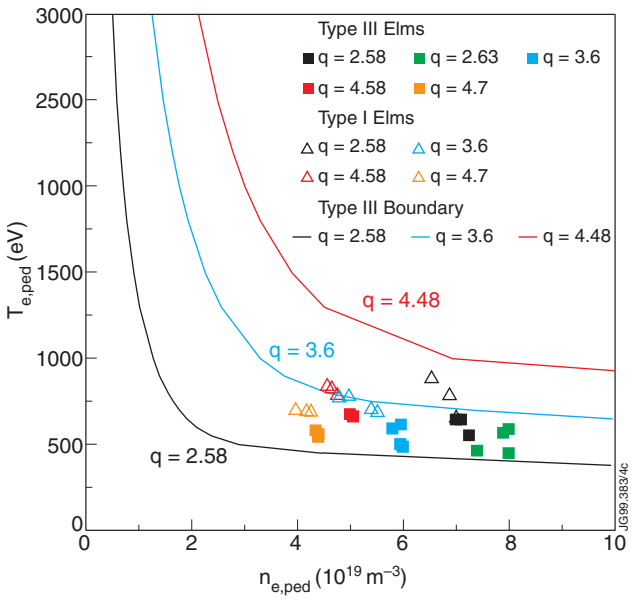

Figure 20: Pedestal n_e-T_e for high density Type I and Type III ELMs in gas scans carried out at different q_{95}.The experimental data in this figure are the same data that were analysed in reference [7]. q_{95} was varied by varying I_p at constant B_t or B_t at constant I_p in separate gas scans.

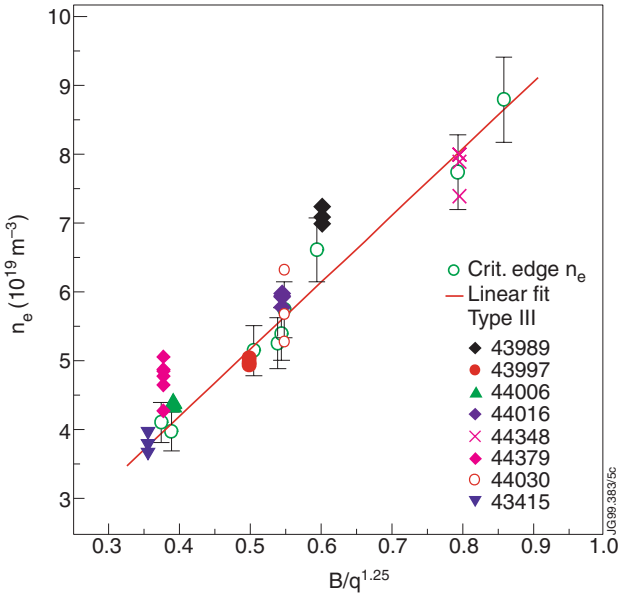

Figure 21: Pedestal density at the Type I-III ELM transition and during Type III ELMs.

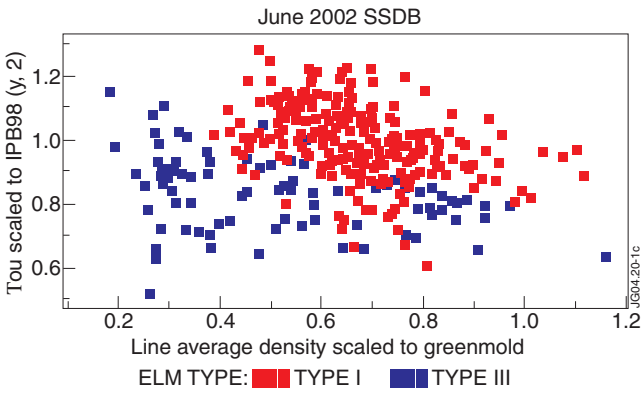

Figure 22: H98(y,2) versus n_e/n_G for Type I (red) and Type III (blue) ELMy H-modes from the database of steady state ELMy H-modes in JET.

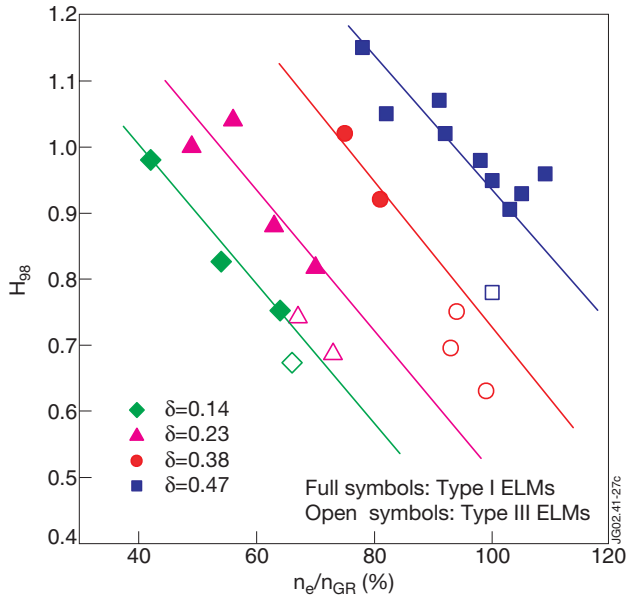

Figure 23: H98(y,2) vs n⁄nG for plasmas with different triangularity. The closed symbols are data for Type I ELMy H-modes, the open symbols for Type III ELMy H-modes[14].

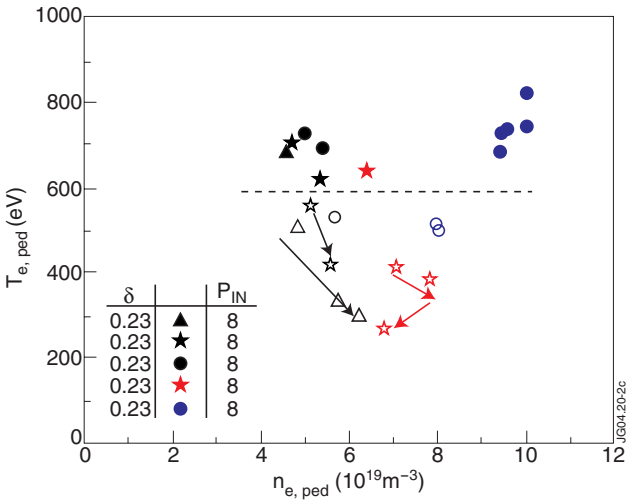

Figure 24: Pedestal Te vs pedestal ne for Type I and Type III ELMy plasmas at high density.
Empty symbols: Type III ELMs Full symbols: Type I ELMs